The Study of pH-Dependent Stability Shows that the TPLH-Mediated Hydrogen-Bonding Network Is Important for the Conformation and Stability of Human Gankyrin

ARTICLE *in* BIOCHEMISTRY · JUNE 2013

Impact Factor: 3.02 · DOI: 10.1021/bi4005717 · Source: PubMed

Published in final edited form as:
Biochemistry. 2013 July 16; 52(28): . doi:10.1021/bi4005717.

The study of pH-dependent stability shows that TPLH-mediated hydrogen-bonding network is important for the conformation and stability of human gankyrin†

Chunhua Yuan[#], **Yi Guo**[§], **Lu Zhu**[§], **Wei Guo**[§], **Anjali Mahajan**[§], **Christopher M. Weghorst**[¶,‡], and **Junan Li**[¶,‡,*]

[#]Campus Chemical Instrument Center, The Ohio State University, Columbus, OH 43210

[§]Ohio State Biochemistry Program, The Ohio State University, Columbus, OH 43210

[¶]Division of Environmental Health Sciences, College of Public Health, The Ohio State University, Columbus, OH 43210

[‡]Comprehensive Cancer Center, The Ohio State University, Columbus, OH 43210

Abstract

Ankyrin repeat (AR) proteins possess a distinctive modular and repetitive architecture, and their global folds are maintained by short-range interactions in terms of primary sequence. In this work, we extended our previous study on the highly conserved TPLH tetrapeptide and investigated the impact of a solvent-exposed histidine residue on the pH-dependent stability of gankyrin, providing further insight into the contribution of the TPLH motif to the tertiary fold of AR proteins. Consisting of seven ARs, gankyrin has five histidine residues in TPLH motifs or its variants, all of which adopt a $H^{\varepsilon 2}$-tautermeric form and are shielded from solvent. By truncating the C-terminal ankyrin repeat (AR7), we exposed H177 in the ^{174}TPLH^{177} of AR6 (the second C-terminal AR) to aqueous environment. We showed that this truncated gankyrin mutant, namely, Gank$^{1\text{-}201}$, was well-folded at a neutral pH with a slightly lower stability with respect to gankyrin wild type (WT). However, unlike gankyrin WT, the stability of Gank$^{1\text{-}201}$ was markedly decreased together with a loss of conformation at a pH slightly below 6.0. It was rationalized that the protonation of the H177 imidazole ring triggered the disruption of the TPLH-mediated hydrogen-bonding network, which in turn led to the loss of conformation and stability. These results together with the work on Q210H mutant nicely explain that the C-terminal AR7 has a ^{207}TPLQ^{210} variant, and are in support of the notion that a string of TPLH/variant, which may arguably act like a zip lock to the elongated AR proteins via intra-/inter-repeat hydrogen-bonding, is important in maintaining the tertiary fold. Additionally, we made rational mutagenesis to introduce extra surface charge on AR7 of gankyrin and demonstrated that G214E and I219D mutations increased the stability of gankyrin while the function remained intact. Taken together, our results indicate that TPLH-mediated hydrogen-bonding network is important for the conformation and stability of human gankyrin, and the C-terminal AR contributes to the conformational stability of gankyrin (AR proteins in general) through shielding this TPLH network from solvent as well as making the surface area more accessible to solvent.

†This work was partly supported by a research grant NIH, R01 CA69472 (J.L.).

*To whom correspondence should be addressed. Tel: 1-614-292-4066. Fax: 1-614-292-4053. li.225@osu.edu.

Support Information Available

The downfield regions of 1D 1H NMR spectra were recorded on Gankyrin WT and Gank1-201 mutant under different pHs to determine the impact of pH on $H^{\varepsilon 2}$ signals of H45, H78, H111, H144, and H177. This material is available free of charge via the Internet at http://pubs.acs.org.

Keywords

gankyrin; ankyrin repeat; TPLH tetrapeptide; conformational stability; pH dependence

Ankyrin repeat (AR) proteins are one of the most abundant repeat protein classes in nature and play vital roles in numerous physiological processes through mediating protein/protein interactions (1–4). Consisting of 33 amino acid residues, an ankyrin repeat exhibits an L-shaped conformation in which two anti-parallel α-helices are followed by a relatively flexible β-loop roughly perpendicular to the helical axes. Multiple L-shaped units in an AR protein are stacked contiguously side-by-side in a nearly linear fashion to form helix-turn-helix bundles (3, 4). Such elongated fold, unlike prevalent globular ones, is maintained by short-range interactions in terms of primary sequence, and the conformational stability is the accumulation of the intrinsic stability of each AR and the interfacial stability between neighboring ARs (4).

One salient feature in an ankyrin repeat is the presence of the conserved TPLH tetrapeptide motif (5, 6). In this motif, the proline residue initiates the first α-helix of the L-shaped unit, while the pair of Thr and His act in concert to form intra-/inter-repeat hydrogen bonds (Figure 1). It is noteworthy that the conserved histidine adopts a $H^{\varepsilon 2}$-tautermeric form and plays a unique role in maintaining the global conformation of an AR protein (6). Briefly, $N^{\delta 1}$ of this histidine is engaged in bifurcated hydrogen bonds with the Thr in the same TPLH motif, whereas protonated $N^{\varepsilon 2}$ acts as a donor to the backbone carbonyl oxygen of the residue immediately preceding the next TPLH motif (6). The occurrence of a string of TPLH motifs, such as in human ankryinR (7) and human gankyrin (8, 9), could conceivably lead to the formation of a large hydrogen-bonding network throughout the repeat stack, thus playing crucial roles in stabilizing the tertiary fold. This notion is supported by our previous studies showing that the TPLH motif contributes substantially to the conformational stability of human gankyrin (10).

Gankyrin is an oncogenic protein involved in cell cycle progression, apoptosis, and proteasomal degradation through binding and modulating the cyclin-dependent kinase 4 (CDK4), pRb (the retinoblastoma susceptible gene product), MDM2 (a protein encoded by murine double minute gene, *mdm2*), and S6 ATPase (11). Among its seven AR units (namely, AR1 to AR7), all but the N-terminal one (AR1) have TPLH motif or a close variant, such as ^{207}TPLQ^{210} in the C-terminal AR unit, AR7. In this example, the highly conserved histidine is replaced with a glutamine residue (6). Unlike the counterpart in the TPLH motif of an internal or N-terminal AR, histidine in the C-terminal AR does not have a hydrogen-bonding acceptor for the protonated $N^{\varepsilon 2}$, and the imidazole ring is expected to be largely solvent exposed, which may not be favored with regard to the conformational stability (10). In this work we investigated the potentially deleterious effect by such a solvent-exposed histidine on the global conformation and stability, aiming at further understanding the structural role of the TPLH motif. We anticipated that the likelihood protonation of the imidazole ring at physiological pH may destabilize the protein *via* impairing the TPLH-mediated hydrogen-bonding network. To address this premise, we generated Q210H mutant, and most importantly, the truncated gankyrin mutant, Gank$^{1\text{-}201}$, in which the entire C-terminal AR (AR7) is removed thus rendering H177 in the ^{174}TPLH^{177} motif of AR6 exposed to the aqueous environment (12). The mutants were then subjected to pH-dependent studies. This work also intertwined with another specific aim that is to investigate the structural and functional role of AR7. Our work is significant in the following. (1) Participation of a $H^{\varepsilon 2}$-tautermeric histidine is a prerequisite for forming a large TPLH-mediated hydrogen-bond network; and this network may act like a zip lock to the elongated fold of AR proteins; (2) Protonation of the participating histidine residue

likely disrupts the above network and triggers perturbations in the conformation and stability; (3) Unlike in *Drosophila melanogaster* Notch ankyrin repeat domain (ARD) (13), the C-terminal AR7 of gankyrin does not have a significant contribution to the global conformational stability but does enhance protein's susceptibility against pH; and (4) we also showed that AR7 of gankyrin is important for MDM2 binding but not CDK4 binding, and G214E and I219D mutations in this repeat significantly increased the conformational stability.

MATERIALS AND METHODS

Protein expression and purification

Human gankyrin was expressed as a glutathione-*S*-transferase (GST) -fusion protein in *Escherichia coli* BL21 (DE3) Codon plus cells (Novagen) as previously described (14). After sonication and centrifugation, the soluble cell lysate was loaded on a reduced glutathione-agarose (G beads) column (Sigma) equilibrated with phosphate-buffered saline (PBS, pH 7.4). Bound GST-gankyrin was eluted out with reduced glutathione (20 mg/mL in PBS) and further purified by a Q Fastflow column (Amersham). To remove the GST tag, 100 units of PreScission protease (2 units/μl; Amersham) were added to GST-gankyrin in PBS. After incubation at 4 °C for 24 h, the protein solution was loaded onto a column of G beads and the flow-through was concentrated and further purified by an S100 column (Pharmacia) equilibrated with 5 mM HEPES, 1 μM EDTA, and 1 mM DTT (pH 7.4). After SDS–PAGE analysis, fractions containing free gankyrin protein were pooled, concentrated, and lyophilized for further analyses. All gankyrin mutants except Q210H were generated using PCR-based site-directed mutagenesis (Stratagene), and were expressed and purified essentially the same as gankyrin wild type (WT).

Gankyrin Q210H was generated using a pET-21d (+)-gankyrin template in which gankyrin was expressed as a C-terminal His6-tagged protein (14). The lysate from bacteria harboring the pET-21d (+)-Q210H was loaded onto a TALON Cobalt affinity column (BD Sciences) and washed with PBS-20 mM imidazole. Bound proteins were eluted using PBS containing 50, 100, 200, and 300 mM imidazole. After SDS-PAGE analysis, fraction containing Q210H were pooled and dialyzed against PBS and the aforementioned HEPES buffer (pH 7.4). Of note, there is virtually no difference in the conformational stabilities of gankyrin wild type proteins purified from both GST-tagged and his6-tagged procedures (data not shown).

Mouse *mdm2* cDNA gene was cloned into pGEX-4T-1 (Amersham) and expressed as a GST -fusion protein in BL21 (DE3) Codon plus cells upon IPTG induction. GST-MDM2 was purified following the same procedure of GST-gankyrin purification as described above. Similarly, GST was purified from BL21 (DE3) Codon plus cells harboring pGEX-4T-1 and used as control in the following pull-down assays.

The CDK4/cyclin D2 holoenzyme was purified from Highfive insect cells (Invitrogen) as described previously (15). Briefly, insect cells were co-infected with baculoviruses expressing human CDK4 and cyclin D2 for 48 h. Upon centrifugation, cells were resuspended in the ice-cold sonication buffer (20 mM Tris-HCl, 100 mM NaCl, 0.1 mM Na_3VO_4, 1 mM NaF, 10 mM β-glycerophosphate, 5mM β-mercaptoethanol, 0.2 mM AEBSF, 5 μg/mL aprotinin, 5 μg/mL leupeptin, pH 7.4) and broken by sonication. Lysates were cleared by centrifugation and loaded on a TALON affinity resin column (BD Sciences; pre-equilibrated with the sonication buffer). After the resin was washed with the sonication buffer and the sonication buffer containing 10 mM imidazole (pH 7.4), respectively, bound CDK4/cyclin D2 holoenzyme was eluted in the sonication buffer containing 50 mM imidazole (pH 7.4) and dialyzed against the kinase buffer (50 mM HEPES, 10 mM $MgCl_2$, 2.5 mM EGTA, 1 mM DTT, 0.1 mM Na_3VO_4, 1 mM NaF, 10 mM β-glycerophosphate,

5mM β-mercaptoethanol, 0.2 mM AEBSF, 5 μg/mL aprotinin, 5 μg/mL leupeptin, pH 7.4). Concentrated aliquots (at about 0.3 mg/mL) were stored at −80 °C before use.

Pull-down assays

To investigate the interaction between GST-gankyrin proteins (including WT and mutants) and the CDK4-cyclin D2 complex, 10 μg of the CDK4-cyclin D2 complex and 25 μg of GST-gankyrin proteins were incubated in 300 μL of PBS (pH 7.4) at 4 °C for 3 h (14). The concentration of CDK4-cyclin D2 and GST-gankyrin were 0.3 and 3.0 μM, respectively. Subsequently, 250 μL of G beads (pre-equilibrated with PBS at 4 °C) was added into the reaction mixture. After incubation at 4 °C for another 4 h, the reaction mixture was loaded onto a spin column (Fisher Scientific), centrifuged at 4 °C, 1000 rpm for 2 min, and washed with PBS three times. G beads-bound proteins were then eluted out using 150 μL of PBS containing reduced glutathione (20 mg/mL) and further analyzed with Western blot using anti-human CDK4 antibody (sc-2006; Santa Cruz Biotechnology) as previously reported (14).

A similar assay was performed to evaluate the potential interaction between MDM2 and free gankyrin proteins except: (1) each reaction mixture contained GST-MDM2 (at about 0.3 μM) and non-tagged gankyrin protein (including WT and mutants; at 3.0 μM); (2) the pull-down products were blotted against anti-human gankyrin polyclonal antibody (PW8325; BIOMOL International).

Circular dichroism (CD) analyses

For guanidinium hydrochlorife (GdnHCl)-induced unfolding, lyophilized gankyrin proteins were dissolved in 10 mM sodium borate buffer (at pH 7.4, 8.4, 6.4, 5.4 as indicated) containing 40 μM DTT and dialyzed against this borate buffer at 4 °C overnight (12). Samples containing about 2.5 μM proteins were incubated with different amounts of guanidinium hydrochloride (GdnHCl, in a stock solution of 8.5 M) on ice overnight and then equilibrated at 20 °C just prior to CD analysis. The rotation at 222 nm was measured on an AVIV 62A DS far-UV spectropolarimeter using a quartz microcell (Helma) of 0.1 cm light pass length, and the exact concentrations of GdnHCl were determined using the refractive index. For each sample, three scans were averaged. The ellipticity at 222 nm, an indicator of the existence of α–helical secondary structure was taken as the measure of the degree of structure present in the protein at each GdnHCl concentration. The following values were obtained on the basis of two-state approximation: ΔG_d^{water} (denaturation free energy in water), $D_{1/2}$ (denaturant concentration at the midpoint of transition), and the slope of m (a constant related to a protein's susceptibility to chemical denaturant).

Heat-induced unfolding experiments were performed using about 10.0 μM proteins in the borate buffer (at indicated pH) with 1 nm bandwidth and a 10 second response time. Thermal melting spectra were recorded at 222 nm by heating from 5 °C to 65 °C (for gankyrin WT and a $Gank^{1\text{-}201}$) or 70 °C (for gankyrin missense mutants) at the rate of 1 °C per minute and a 1 °C interval followed by cooling down to 5 °C at the same rate. T_m was defined as the temperature at the midpoint of transition.

NMR experiments

Eight NMR samples were prepared containing 0.2 mM either WT or $Gank^{1\text{-}201}$, 5 mM HEPES, 1 μM EDTA, 1 mM DTT in 90% H_2O/10% D_2O (15). The pH was adjusted to 5.4, 6.4, 7.4, and 8.4, respectively. 1D ^1H NMR and 2D NOESY (200 ms mixing time) experiments were performed at 25 °C on a Bruker DRX-600 equipped with a cryoprobe using WATERGATE (16) for the water suppression.

RESULTS

Q210H mutant tends to aggregate and precipitate in solution

Previous studies in our laboratory have demonstrated that the conformation of gankyrin is stabilized by the TPLH-mediated hydrogen-bonding network, in which the highly conserved histidine residues play pivotal roles. Interestingly, in the C-terminal AR of gankyrin (AR7), a glutamine residue replaces the conserved histidine in the aforementioned tetrapeptide motif (^{207}TPLQ^{210}), which is assumed to "close" the hydrogen-bonding network to stabilize the global structure. To address this premise, we introduced histidine residue in the C-terminal ^{207}TPLQ^{210} and evaluated the biochemical and biophysical properties of the resultant Q210H mutant protein. Unlike gankyrin WT and other missense mutants investigated in this work as well as our previous studies (10, 17), Q210H aggregated to a considerable extent during the expression and purification process, and the protein obtained easily precipitates at a concentration of around 0.2 mM. It was noticed that precipitation became more severe at a pH lower than 6.0. While the mechanisms underlying such poor solubility remain to be elucidated, it is important to note that Q210H mutation occurs in the middle of the first helix of AR7, which is somewhat abbreviated (in comparison with its counterparts in other ARs) due to the presence of Gly tandem (G214 and G215) at the end of the first helix (Figure 3). In regard to the low solubility of Q210H, folding/unfolding experiments were performed at an extremely low concentration of about 5 μM using CD spectroscopy. All data were fitted to a biphasic model between native and completely unfolded proteins (Figure 2) (4). Table 1 lists the values of ΔG_d^{water}, $D_{1/2}$, and the slope m obtained in GdnHCl-induced unfolding. Under physiological pH (pH 7.4), the ΔG_d^{water} value of Q210H was 2.32 kcal*mol^{-1}, which is moderately lower than that of gankyrin WT (2.72 kcal*mol^{-1}). Consistently, in heat-induced unfolding, the T_m value of Q210H at pH 7.4 was 49.9 °C, slightly lower than the corresponding one (51.2 °C) for gankyrin WT. These results suggest that Q210H mutation moderately destabilizes the global structure of gankyrin under physiological pH. However, further pH-dependent stability studies on Q210H were hindered most likely due to its poor solubility at acidic pHs. While the ΔG_d^{water} and T_m values of Q210H at pH 8.4 (1.97 kcal*mol^{-1} and 49.0 °C, respectively) were only marginally lower than the corresponding values at pH 7.4. we failed to obtain the denaturation curves at pH 5.4 and 6.4 due to extremely poor CD signals, which may be ascribed to precipitation and/or a complete loss of the secondary structure of Q210H at acidic pHs.

Attempts to study Q210H by NMR experiments, such as 2D NOESY to tentatively assign H$^{\varepsilon 2}$ of H210, were also compromised by this mutant's tendency to severe aggregation at a concentration, i.e. 0.2 mM, necessitated for NMR analyses. Only 1D ^{1}H NMR spectra of Q210H at pH 5.4, 6.4, 7.4, and 8.4 were recorded at extremely low concentrations (< 0.1 mM). As shown in Figure 4, the mutant at neutral pH does possess good chemical shift dispersion with weak signals in the 10~ 12 ppm downfield region, indicative of a preservation of tertiary structure. However, the mutant becomes less structured at pH 5.4 evidenced by the disappearance of those downfield signals, likely attributed to the unfavorable solvent exposure of H210.

Taken together, it is arguably safe to state that Q210H mutation impairs some biophysical properties of gankyrin, such as the tendency to aggregate, which may have a bearing on the stability of the global structure. However, the severe aggregation tendency of Q210H mutant complicated our endeavor to explore the pH dependency of its conformational stability. Therefore, we turned to constructing Gank$^{1\text{-}201}$ mutant, in which AR7 is removed thus exposing H177 in ^{174}TPLH^{177} motif of AR6 to solvent.

Gank$^{1-201}$ shows a transition point around pH 6.0 for a significant loss of conformational stability by CD analysis

Both Gank$^{1-201}$ and WT were subjected to parallel experiments of chemical- and thermal-denaturation at pH 5.4, 6.4, 7.4, and 8.4 monitored by CD spectroscopy (12). As shown in Table 1 and Figure 2, Gank$^{1-201}$, the truncated mutant, only exhibited a slight or moderate change of 0.62 kcal*mol^{-1} in conformational stability with respect to gankyrin WT at neutral pH. Moreover, the ΔG_d^{water} and m values of Gank$^{1-201}$ at pH 6.4 and 8.4 were comparable with the corresponding values of Gank$^{1-201}$ at neutral pH, indicating that Gank$^{1-201}$ is relatively stable in the range of pH 6.4 – 8.4. However, the unfolding behavior of Gank$^{1-201}$ changed dramatically at pH 5.4, which can be appreciated by a more sigmoidal denaturation curve (Figure 2A). Even though there is no representative baseline at the native state in the unfolding of Gank$^{1-201}$ at pH 5.4, its apparent ΔG_d^{water} value from the two-state transition approximation was around 0.5 kcal*mol^{-1}, indicating that this mutant becomes only marginally stable at pH 5.4. Consistently, at pH 5.4, Gank$^{1-201}$ is much less structured in the presence of high concentrations of the denaturant (GdnHCl) with an apparent $D_{1/2}$ value of 0.42 M. In comparison, the $D_{1/2}$ value of Gank$^{1-201}$ at pH 6.4 is 1.44 M. Therefore, Gank$^{1-201}$ likely undergoes dramatic conformational changes from pH 6.4 to 5.4. In contrast, slightly acidic pH appeared to have little influence on gankyrin WT, which did not show any significant changes in ΔG_d^{water}, m and $D_{1/2}$ in the range of pH 5.4 – 8.4 (Table 1).

The above notion is further supported by heat-induced unfolding studies (Figure 2B). First, the heating and cooling curves of gankyrin WT and Gank$^{1-201}$ are virtually superimposable, and the T_m values determined from the heating and cooling curves are within 1 °C, indicating that the proteins are at thermodynamic equilibrium and the thermo-induced folding/unfolding is reversible (data not shown). Secondly, Gank$^{1-201}$ and gankyrin WT have comparable thermo-stability around neutral pH, confirming the result of chemical-induced unfolding that AR7 does not have a significant impact on the conformational stability of gankyrin. However, while the T_m of gankyrin WT are within seven degree of difference in the pH range studied, Gank$^{1-201}$ showed a twice larger of the T_m differences due to a significant lower value at pH 5.4, further indicating physical-chemical changes of Gank$^{1-201}$ under this pH condition. Taken together, while we do not attempt to over-interpret small or modest changes of ΔG_d^{water} and T_m in both gankyrin WT and Gank$^{1-201}$, it is safe to draw the conclusion that the removal of the C-terminal AR renders the global structure more susceptible to acidic circumstances with a turning point roughly around pH 6.0.

Gank$^{1-201}$ retains a global fold around neutral pH but loses some structures at a pH below 6.0 evidenced from NMR studies

We subsequently revealed that the decreased stability of Gank$^{1-201}$ at pH 5.4 is associated with the loss of conformation. Firstly, the mutant was subjected to the studies of 1D ^{1}H NMR and 2D ^{1}H homonuclear NOESY at pH 7.4 (Figure 5). The large ^{1}H chemical shift dispersion in the aliphatic (e.g. upfield resonances at −0.59, −0.39, and −0.13 ppm) and the amide regions (e.g. downfield resonances at 10.54, 10.60, and 10.83 ppm) together with the high density of NOE cross peaks suggested that this mutant was well folded under this pH condition. Secondly, the analysis of the downfield region of NOESY spectrum led to the tentative assignment of the five distinctive H$^{\varepsilon 2}$ resonances of histidine in TPLH/variants, which are sensitive to the formation of hydrogen-bonding network and have been used as a convenient measure of tertiary fold (Figure 5A) (6, 10). Consistent with the modular feature of tertiary fold, the perturbations of H$^{\varepsilon 2}$ chemical shifts with respect to the counterparts in gankyrin WT followed the rank order of H177 (0.17 ppm) > H144 (0.09 ppm) ~ H111 (−0.09 ppm) > H78 (0.02 ppm) ~ H45 (0.00 ppm). These resonances also displayed comparable NOE patterns to those corresponding ones in WT, indicating the preservation of

TPLH-mediated hydrogen-bonding network. And lastly, 1D ^{1}H NMR was performed to monitor those tractable $H^{\varepsilon 2}$ resonances at pH 5.4, 6.4 and 8.4. Data collected immediately upon titration showed little changes (Supplementary Material). However, after incubation at room temperature for a week, the sample at pH 5.4 but not at higher pH revealed dramatic changes that those distinguished downfield $H^{\varepsilon 2}$ signals disappeared with concurrent loss of amide ^{1}H chemical shift dispersion (Figure 5B). Even though residual structures persist evidenced by residual upfield resonances around 0 ppm, Gank$^{1\text{-}201}$ indeed is of significant less structured at a pH below 6.0. These observations on Gank$^{1\text{-}201}$ are in sharp contrast with those in the parallel experiments performed on WT, which has virtually no changes in the ^{1}H NMR, including the downfield region concerning the $H^{\varepsilon 2}$ signals (Figure 5C). Taken together, Gank$^{1\text{-}201}$ shows vulnerable pH-dependent conformation and stability as has been anticipated.

Introducing charged residues into the C-terminal AR of gankyrin stabilized the global structure

Our studies on Gank$^{1\text{-}201}$ as described above demonstrate that AR7 functions to shield the internal ARs from aqueous environment thus increasing the resistance of the global structure to pH. However, it is interesting to explore whether or how AR7 itself directly contributes to the conformational stability of the global structure. Even though gankyrin has the ΔG_{d}^{water} value of 2.72 kcal*mol^{-1} and is more stable than some small AR proteins, such as P16^{INK4A} (4 ARs) and P18^{INK4C} (5ARs) (12), its behavior in GdnHCl-induced unfolding is significantly different from that of *Drosophila melanogaster* Notch ankyrin repeat domain (ARD), another well-studied AR protein consisting of seven ARs (18). Notch ARD was reported to have a conformational stability of 8.03 kcal*mol^{-1} in GdnHCl-induced unfolding and the C-terminal AR7 contributed significantly to the global stability as evidenced by a decrease of 3.89 kcal*mol^{-1} upon the removal of AR7 (19). In contrast, the removal of AR7 in gankyrin only brought about a slight or moderate change of 0.62 kcal*mol^{-1} in conformational stability. Based on the sequence homology analysis using ClustalW (www.expasy.org) (Figure 3), it was noticed that there are comparatively more polar residues at the C-terminus capping repeat of Notch ARD, some of which (R186, E191, R192, and D196) are present on the surface. Presumably, the considerably more surface charges enhance the stability of Notch ARD by making the C-terminal surface more hydrophilic. We therefore made the corresponding substitutions L209R, G214E, G215R, I219D, and G214E/I219D together with two histidine mutations G217H and L218H, and evaluated the mutagenic effect on protein stability.

As shown in Figure 6, all of the mutant proteins exhibit biphasic transitions in GdnHCl- and heat-induced unfolding, indicating that the aforementioned substitutions do not impair the cooperative nature of gankyrin unfolding. The fitting results are summarized in Table 1. Briefly, the values of L209R and G215R are comparable to that of gankyrin WT, whereas G214E and I219D show considerable increase of 1.9 and 2.6 kcal*mol^{-1}, respectively, in the ΔG_{d}^{water}, indicating that G214E and I219D mutations substantially increase the conformational stability. Interestingly, the ΔG_{d}^{water} value of the double mutant, G214E/I219D is almost identical to that of G214E, suggesting that the effects of G214E and I219D are not additive. These findings are further supported by results from heat-induced unfolding (Table 1). Finally, Notch ARD has two histidine residues in the C-terminal AR turn. The corresponding mutations G217H and L218H would introduce a solvent-exposure histidine to the gankyrin C-terminal AR7. However, neither mutation lowers the conformational stability at neutral pH, suggesting that a solvent-exposed histidine in the terminal AR does not intrinsically destabilize the gankyrin.

Mutations and truncation of the C-terminal AR7 did not impair gankyrin's CDK4 binding but truncation abolished its MDM2 binding

We used the pull-down assay to assess the mutagenic effect on the CDK4-binding and MDM2-binding abilities (11). When GST-tagged gankyrin proteins, including WT, Gank$^{1\text{-}201}$, and AR7 point mutants, were incubated with the CDK4-cyclin D2 holoenzyme, CDK4 was detected in all of the pull-down products but not in the negative control using GST itself (Figure 7A), indicating that all of the aforementioned gankyrin proteins are able to bind to CDK4 (14). Since the amounts of CDK4 in the pull-down products are comparable by visual inspection between each individual mutant and the WT, it is concluded that AR7 has minimal impact on the binding of gankyrin to CDK4, consistent with our previous finding that the first four ARs of gankyrin are sufficient for CDK4 binding and modulating (14).

It has been also reported that the AR7 of gankyrin may be involved in binding to MDM2, a key component in the P53 pathway (11, 20). A similar pull-down assay was performed on the reaction mixtures containing GST-MDM2 and gankyrin proteins (Figure 7B). First, under the experimental conditions, gankyrin WT was present in the pull-down product from the GST-MDM2/WT reaction mixture but absent in the one from the GST/WT mixture, indicating that gankyrin specifically interacts with MDM2. Secondly, among all of the reaction mixtures containing GST-MDM2 and AR7 point mutants, gankyrin proteins (WT or point mutants) were detected in the pull-down products, implying that these C-terminal AR7 mutants remained functional in binding to MDM2. However, we failed to detect Gank$^{1\text{-}201}$ in the pull-down product from the GST-MDM2/Gank$^{1\text{-}201}$ mixture. Since this truncated mutant is able to react with the polyclonal anti-gankyrin antibody used in this assay (data not shown), the result indicates that the removal of the entire C-terminal AR significantly impaired or even abolished its MDM2-binding ability.

DISCUSSION

Out of a variety of TPLH-containing AR proteins, gankyrin was chosen as a model in our current study for the following reasons: first, both the structure and function of gankyrin have been extensively investigated; secondly, the modular structure of gankyrin is of considerable resiliency as evidenced by previous findings that gankyrin retains the tertiary fold and CDK4-binding ability upon the introduction of missense mutations and the removal of up to three ARs at the C-terminus (14). The current study extended previous effort to address the important structural role of the conserved TPLH motif for an AR protein. The following discussion will be based on Gank$^{1\text{-}201}$ since more comprehensive results were obtained with respect to Q210H.

Both gankyrin WT and Gank$^{1\text{-}201}$ have close theoretical p*I* values (5.71 and 5.45, respectively) (12), indicating that there is no significant difference in net charge at physiological pH. As shown in Table 1, the stability of gankyrin WT increases from 2.65 kcal*mol^{-1} to 3.55 kcal*mol^{-1} as pH decreases from 8.4 to 5.4. Apparently, the correlation between the stability of gankyrin WT and pH is consistent with the Linderstrom-Lang model (21) that a protein tends to be more stable as pH approaches to the isoelectric point (p*I*), at which the unfavorable electrostatic interactions resulting from an excess of either positive or negative charges is minimized. Similar observation has been reported in an optimized *de novo* designed 4-ANK protein (22). In comparison, Gank$^{1\text{-}201}$ exhibits increasing stability as pH decreases from 8.4 to 6.4 (1.95, 2.10, 2.45 kcal*mol^{-1} at pH 8.4, 7.4, 6.4, respectively), but undergoes dramatic decrease in stability at pH 5.4 (0.55 kcal*mol^{-1}). Clearly, the Linderstrom-Lang model cannot fully account for the pH dependence of Gank$^{1\text{-}201}$ in stability. The change of pH susceptibility of Gank$^{1\text{-}201}$ strongly indicates that some significant chemical/physical changes are triggered by ionization of titratable groups around

pH 6.0. Since histidine is the only amino acid with a pK_a of its side chain in the physiologically relevant pH range, the candidates responsible for the aforementioned change in pH susceptibility can be narrowed down to nine histidine residues in gankyrin. Among them, H177 is the only one that is directly impacted by the truncation of AR7. In gankyrin WT, H177 is largely shielded from solvent like a typical histidine in an internal TPLH. However, the removal of the C-terminal capping repeat (AR7) would increase the solvent-accessibility of the side chain of H177 from roughly 10% to 50% (assuming that potential structural rearrangement is negligible), which may partially contribute to the discrepancy between gankyrin WT and Gank$^{1\text{-}201}$ in thermodynamic properties.

The impact of H177 on conformation and stability of Gank$^{1\text{-}201}$ bears structural implication. First, a newly introduced histidine in the C-terminus does not necessarily cause destabilizing effect as exemplified by two C-terminal AR7 point mutants G217H and L218H. Secondly, the change in the electrostatic status of a solvent-exposed histidine does not necessarily induce dramatic changes in the conformational stability, as H137 is present in the AR4-AR5 loop of both gankyrin WT and Gank$^{1\text{-}201}$ and its side chain is solvent-exposed to the extent of more than 70%. Thus, as has been anticipated, the observation can only be rationalized in the context of the TPLH-mediated hydrogen-bonding network. One may imagine such a scenario that at a pH below 6, H177 in Gank$^{1\text{-}201}$ will gradually shift to a protonated form as described by the Henderson–Hasselbalch equation, bearing $N^{\delta 1}$-H and $N^{\varepsilon 2}$-H bonds in the imidazole ring and a positive charge distributed between $N^{\delta 1}$ and $N^{\varepsilon 2}$. This change would in turn weaken the hydrogen bonds of T174 H^{N}-H177 $N^{\delta 1}$ and T174 $H^{\gamma 1}$-H177 $N^{\delta 1}$, and eventually trigger the loss of the hydrogen bonds mediated by ^{174}TPLH^{177} (6, 10). Such perturbation will induce a ripple effect on the ^{141}TAMH^{144} of the preceding repeat AR5, as the hydrogen bond between N173 O and H144 $H^{\varepsilon 2}$ is likely perturbed. Consequently, the perturbation propagates through the entire repeat stack and ultimately leads to the loss of the TPLH-mediated hydrogen-bonding network and even the global fold. The result on Q210H also appears to support this scenario.

Due to the lack of long-range interactions (3, 4), it is conceived that the TPLH-mediated hydrogen-bonding network plays important roles in maintaining the elongated tertiary fold of AR proteins. Presumably, the strings of TLPH might act like a “zip lock” to the repeat stack *via* the intra-/inter-repeat hydrogen bonds, complementing to the strong hydrophobic interaction between adjacent repeats. In such a model, the tautermeric state of histidine in the TPLH motif is critical, and relatively small shifts in pH around pK_a may lead to unzipping the tertiary fold if any of participating histidines is exposed to aqueous environment. In addition, at the C-terminal AR, a variant in place of histidine would be needed to cap the “zip lock”, i.e. the TPLH-mediated hydrogen-bonding network. Interestingly, there exists a glutamine (Gln) residue in ^{207}TPLQ^{210} of AR7, the C-terminal AR of gankyrin, which is capable of forming reciprocal hydrogen bonds with T207 while having a pK_a far from physiological range. Similar substitutions at the C-terminal AR have been observed in other AR proteins such as ^{252}SPYQ^{255} in IκBα (5), ^{769}TPLA^{772} in human ankyrinR (7), and TPLD or TPQD in a couple of Bcl-3 homologs (23).

The sequence variation in the TPLH motif in the C-terminal AR also implies that even though there is a consistent pattern of key residues in the consensus sequence of AR motifs to retain the characteristic helix-turn-helix conformation, there is considerable sequence divergence in AR motifs, especially terminal repeats to adapt to the aqueous environment. Unlike an internal AR that has interfacial interactions with neighboring ARs from both sides and tends to have two hydrophobic surfaces, a terminal AR is two-faced: a hydrophobic “inner” surface interacting with the penultimate AR and a hydrophilic “outer” surface accessible to the aqueous environment. Apparently, a more hydrophilic “outer” surface of the C-terminal AR may favor its “capping” effect as well as the global stability. As

previously demonstrated (24), a few mutations in the C-terminal AR could significantly improve the stability a de novo designed AR protein. We here show that by introducing charged residues at appropriate position in the C-terminal AR, we could also improve the stability of a naturally occurred AR protein. The difference in stability change for the four mutants could be explained from the structural point of view. L209, G214, and I219 are positioned in the "inner" helix, the turn, and the "outer" helix of the C-terminal AR, respectively. Accordingly, L209 faces the "outer" helix of the penultimate AR and contribute to those "hydrophobic" interfacial interactions with the side chains of K220 and L221 (Figure 3C). Thus, introducing a charged residue through L209R substitution in such "hydrophobic" microenvironment is not thermodynamically favored. In contrast, I219 is directly exposed to the aqueous environment, and substitutions like I219D would enable the C-terminal AR more solvent accessible thus positively influencing the stability of the global structure. So does the substitution of G214E, which introduced a negatively-charged side chain in the turn region and increased the aqueous accessibility. In fact, the percentages of the solvent accessible surface are roughly 32% and 55%, respectively, for the bulky hydrophobic side chains of L209 and I219 (Figure 3D). Interestingly, all these four C-terminal mutants retained CDK4-binding and MDM2-binding abilities comparable to those of gankyrin WT. Therefore, C-terminal substitutions such as G214E can stabilize the global structure of gankyrin but brings about little perturbation to its physiological function. This may be of significance in protein engineering of AR proteins, that is, we can modify those residues far away from the functionally important regions in an AR protein to enhance stability without compromising its function.

It is also worthwhile to note that many AR proteins do not have a string of TPLH motifs (10). In such case, the aforementioned TPLH-mediated hydrogen-bonding network does not exist, and the stability of these AR proteins should be ascribed to the hydrophobic interaction network across the molecule as well as other undefined mechanisms. In addition, it has been reported that two designed AR proteins consisting of three and four identical repeats of consensus sequence, respectively, retain very high stabilities even under acidic pH. On one hand, consensus sequence should result in more optimized hydrophobic interactions between neighboring repeats; and these two proteins may have overcome less ideal or even the loss of TPLH-mediated hydrogen bonding network to retain a global fold. On the other hand, the crystallographic structures of these two designed AR proteins revealed a ring flip of the imidazole ring around C^{β}-C^{γ} bond ($\chi 2 \sim -90°$) (24) in comparison to gankyrin and another de novo designed AR protein (25). The ring flip conformation precludes a hydrogen-bond between His $N^{\varepsilon 2}$ and the carbonyl oxygen of the residue His (+30), suggesting that the TPLH-mediated hydrogen bonding network in these two design AR proteins has been perturbed at the low pH if still existing, and may not be the primary factor contributing to the high stabilities of these two proteins at low pH. Lastly, the pH-dependence of conformational stability attributed to histidine has been observed in other proteins (26).

In conclusion, AR7 of gankyrin is not essential to maintain a tertiary fold of AR1-AR6, but it moderately stabilizes the global structure as well as increases its susceptibility against acidic pHs by shielding the internal hydrophobic interactions and TPLH-mediated hydrogen-bonding network from the aqueous environment. The current work is valuable for understanding the unique biophysical properties of gankyrin (AR proteins in general) and for novel AR protein design.

Supplementary Material

Refer to Web version on PubMed Central for supplementary material.

Abbreviations

AR	ankyrin repeat
CD	circular dichroism
CDK4	cyclin-dependent kinase 4
GdnHCl	guanidinium hydrochloride
MDM2	a protein encoded by the murine double minute (*mdm2*) oncogene
NMR	Nuclear Magnetic Resonance
NOESY	Nuclear Overhauser effect Spectroscopy
Notch ARD	the ankyrin repeat domain in Notch
WT	wild type

References

1. Bork P. Hundreds of ankyrin-like repeats in functionally diverse proteins: mobile modules that cross phylahorizontally? Proteins: Structure, Functions, and Genetics. 1993; 17:363–374.
2. Sedgwick SG, Smerdon SJ. The ankyrin repeat: a diversity of interactions on a common structural framework. Trends Biochem Sci. 1999; 24:311–316. [PubMed: 10431175]
3. Mosavi LK, Cammett TJ, Desrosiers DC, Peng Z-Y. The ankyrin repeat as molecular architecture for protein recognition. Protein Sci. 2004; 13:1435–1448. [PubMed: 15152081]
4. Li J, Mahajan A, Tsai MD. Ankyrin repeat: a unique motif mediating protein-protein interactions. Biochemistry. 2006; 45:15168–15178. [PubMed: 17176038]
5. Jacobs MD, Harrison SC. Structure of an IκBα/NF-κB complex. Cell. 1998; 95:749–758. [PubMed: 9865693]
6. Yuan C, Li J, Mahajan A, Poi MJ, Byeon IL, Tsai M-D. Solution structure of the human oncogenic protein gankyrin containing seven ankyrin repeats and analysis of its structure-function relationship. Biochemistry. 2004; 43:12152–12161. [PubMed: 15379554]
7. Michaely P, Tomchick DR, Machius M, Anderson RG. Crystal structure of a 12 ANK repeat stack from human ankyrinR. EMBO J. 2002; 21:6387–6396. [PubMed: 12456646]
8. Krzywda S, Brzozowski AM, Higashitsuji H, Fujita J, Welchman R, Dawson S, Mayer RJ, Wilkinson AJ. The crystal structure of gankyrin, an oncoprotein found in complexes with cyclin-dependent kinase 4, a 19S proteasomal ATPase regulator, and the tumor suppressors of Rb and p53. J Biol Chem. 2004; 279:1541–1545. [PubMed: 14573599]
9. Manjasetty BA, Quedenau C, Sievert V, Bussow K, Niesen F, Delbruck H, Heinemann U. X-ray structure of human gankyrin, the product of a gene linked to hepatocellular carcinoma. Proteins: Structure, Functions, and Genetics. 2004; 55:214–217.
10. Guo Y, Yuan C, Tian F, Huang K, Weghorst CM, Li J. Contributions of conserved TPLH tetrapeptides to the conformational stability of ankyrin repeat proteins. J Mol Biol. 2010; 399:168–181. [PubMed: 20398677]
11. Li J, Guo Y. Gankyrin oncoprotein: structure, function, and involvement in cancer. Current Chemical Biology. 2010; 4:13–19.
12. Guo Y, Mahajan A, Yuan C, Joo S-H, Weghorst CM, Tsai M-D, Li J. Comparison of the conformational stability of cyclin-dependent kinase (CDK) 4-interacting ankyrin repeat (AR) proteins. Biochemistry. 2009; 48:4050–4062. [PubMed: 19320462]
13. Bradley CM, Barrick D. Limits of cooperativity in a structurally modular protein: response of the Notch ankyrin repeat domain to analogous substitutions in each repeat. J Mol Biol. 2002; 324:373–386. [PubMed: 12441114]
14. Li J, Tsai MD. Novel insights into the INK4-CDK4/6-Rb pathway: counter action of gankyrin against INK4 proteins regulates the CDK4-mediated phosphorylation of Rb. Biochemistry. 2002; 41:3977–3983. [PubMed: 11900540]

15. Byeon IJ, Li J, Ericson K, Selby TL, Tevelev A, Kim HJ, O'Maille P, Tsai M-D. Tumor suppressor p16INK4A: determination of solution structure and analyses of its interaction with cyclin-dependent kinase 4. Mol Cell. 1998; 1:421–431. [PubMed: 9660926]

16. Sklenar V, Piotto M, Leppik R, Saudek V. Gradient-tailored water suppression for 1H-15N HSQC experiments optimized to retain full sensitivity. J Magn Reson Ser. 1993; 102:241–245.

17. Mahajan A, Guo Y, Yuan C, Weghorst CM, Tsai M-D, Li J. Dissection of protein-protein interaction and CDK4 inhibition in the oncogenic versus tumor suppressing functions of gankyrin and p16. J Mol Biol. 2007; 373:990–1005. [PubMed: 17881001]

18. Zweifel ME, Barrick D. Studies of the ankyrin repeats of the Drosophila melanogaster Notch receptor. 1 Solution conformational and hydrodynamic properties. Biochemistry. 2001; 40:14344–14356. [PubMed: 11724546]

19. Zweifel ME, Barrick D. Studies of the ankyrin repeats of the Drosophila melanogaster Notch receptor. 2 Solution stability and cooperativity of unfolding. Biochemistry. 2001; 40:14357–14367. [PubMed: 11724547]

20. Higashitsuji H, Higashitsuji H, Itoh K, Sakurai T, Nagao T, Sumitomo Y, Masuda T, Dawson S, Shimada Y, Mayer RJ, Fujita J. The oncoprotein gankyrin binds to MDM2/HDM2, enhancing ubiquitylation and degradation of p53. Cancer Cell. 2005; 8:75–87. [PubMed: 16023600]

21. Linderstrom-Lang KU. On the ionisation of proteins. CR Trav Lab Carlsberg. 1924; 15:1–29.

22. Mosavi LK, Peng Z-Y. Structure-based substitutions for increased solubility of a designed protein. Protein Eng. 2003; 16:739–745. [PubMed: 14600203]

23. Michel F, Soler-Lopez M, Petosa C, Cramer P, Siebenlist U, Muller CW. Crystal structure of the ankyrin repeat domain of Bcl-3: a unique member of the IkappaB protein family. EMBO J. 2001; 20:6180–6190. [PubMed: 11707390]

24. Kramer MA, Wetzel SK, Pluckthun A, Mittl PR, Grutter MG. Structural determinants for improved stability of designed ankyrin repeat proteins with a redesigned C-capping module. J Mol Biol. 2010; 404:381–391. [PubMed: 20851127]

25. Mosavi LK, Minor DL, Peng ZY. Consensus-derived structural determinants of the ankyrin repeat motif. Proc Natl Acad Sci USA. 2002; 99:16029–16034. [PubMed: 12461176]

26. Schowalter RM, Chang A, Robach JG, Buchholz UJ, Dutch RE. Low pH triggering of human metapneumovirus fusion: essential residues and importantance in entry. J Virol. 2009; 83:1511–1522. [PubMed: 19036821]

27. Pace CN. Determination and analysis of urea and guanidine hydrochloride denaturation curves. Methods Enzymol. 1986; 131:266–280. [PubMed: 3773761]

28. Koradi R, Billeter M, Wuthrich K. MOLMOL: a program for display and analysis of macromolecular structures. J Mol Graphics. 1996; 14:51–55.

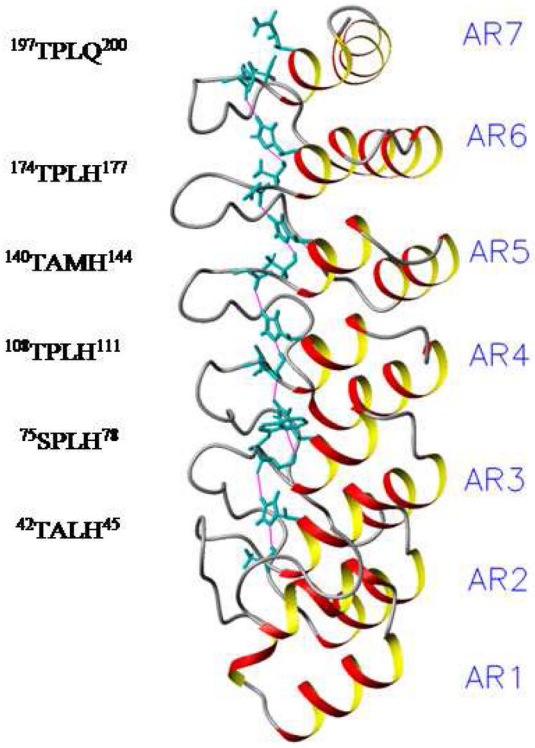

Figure 1. Ribbon diagram of gankyrin showing the side chains of Thr (Ser) and His (Gln) in TPLH motifs as well as the heavy atoms of His (+30) in cyan color

The hydrogen bonds between Thr $H^{\gamma 1}$ (Ser H^{γ}) and His $N^{\delta 1}$ and between His $H^{\varepsilon 2}$ and His (+30) O are highlighted by the solid line in magenta color, which are part of the TPLH-mediated hydrogen bonding network (6, 10).

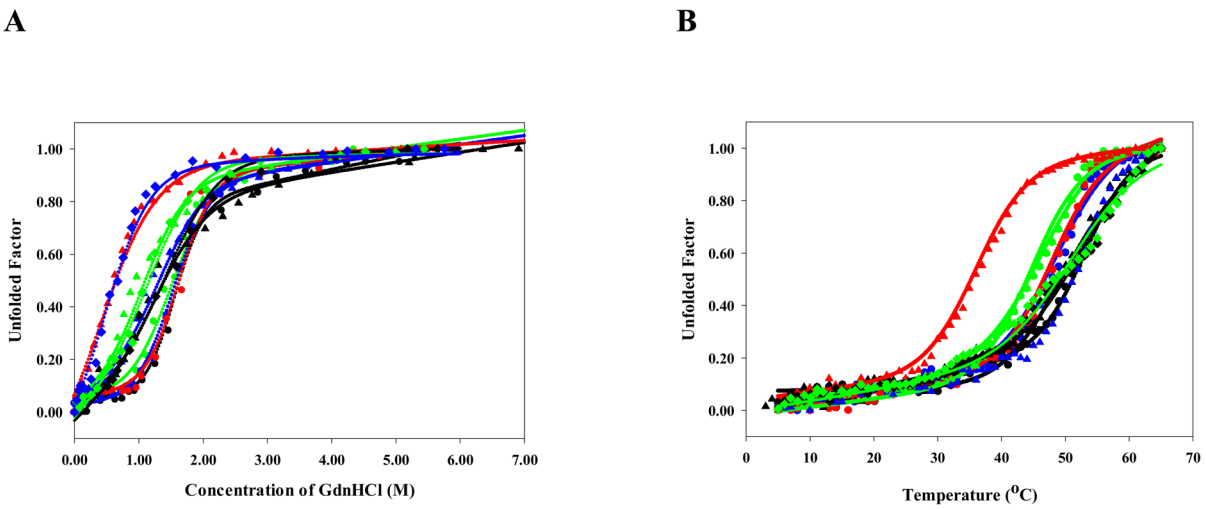

Figure 2. Evaluation of the conformational stabilities of WT, Gank$^{1-201}$, and Q210H under different pHs

A, Chemical-induced unfolding of gankyrin and Gank$^{1-201}$. Samples were incubated with different amounts of GdnHCl on ice overnight. The ellipticity at 222 nm was monitored by far-UV CD (190–260 nm) at 20 °C. The fraction unfolded, defined as (the ellipticity at 222 nm at a denaturant concentration-the ellipticity at 222 nm at the native state)/(the ellipticity at 222 nm at the fully unfolded state-the ellipticity at 222 nm at the native state), was plotted against the GdnHCl concentration. **B,** Heat-induced unfolding of gankyrin, Gank$^{1-201}$, and Q210H. Thermal melting spectra were recorded at 222 nm by heating from 5 °C to 65 °C with a rate of 1°C per minute and a 1 °C interval. Tm, the temperature at the midpoint of transition, was obtained through fitting the melting curve to a two-state transition model. In both **A** and **B,** solid circles, triangles, and diamonds represent experimental data for gankyrin WT, Gank$^{1-201}$, and gankyrin Q210H, respectively, and different colors indicate different pHs: black, pH 7.4; green, pH 8.4; blue, pH 6.4; red, pH 5.4. The unfolding parameters were derived through a two-state transition approximation (27) and listed in Table 1. The dotted lines represent the fitting curves.

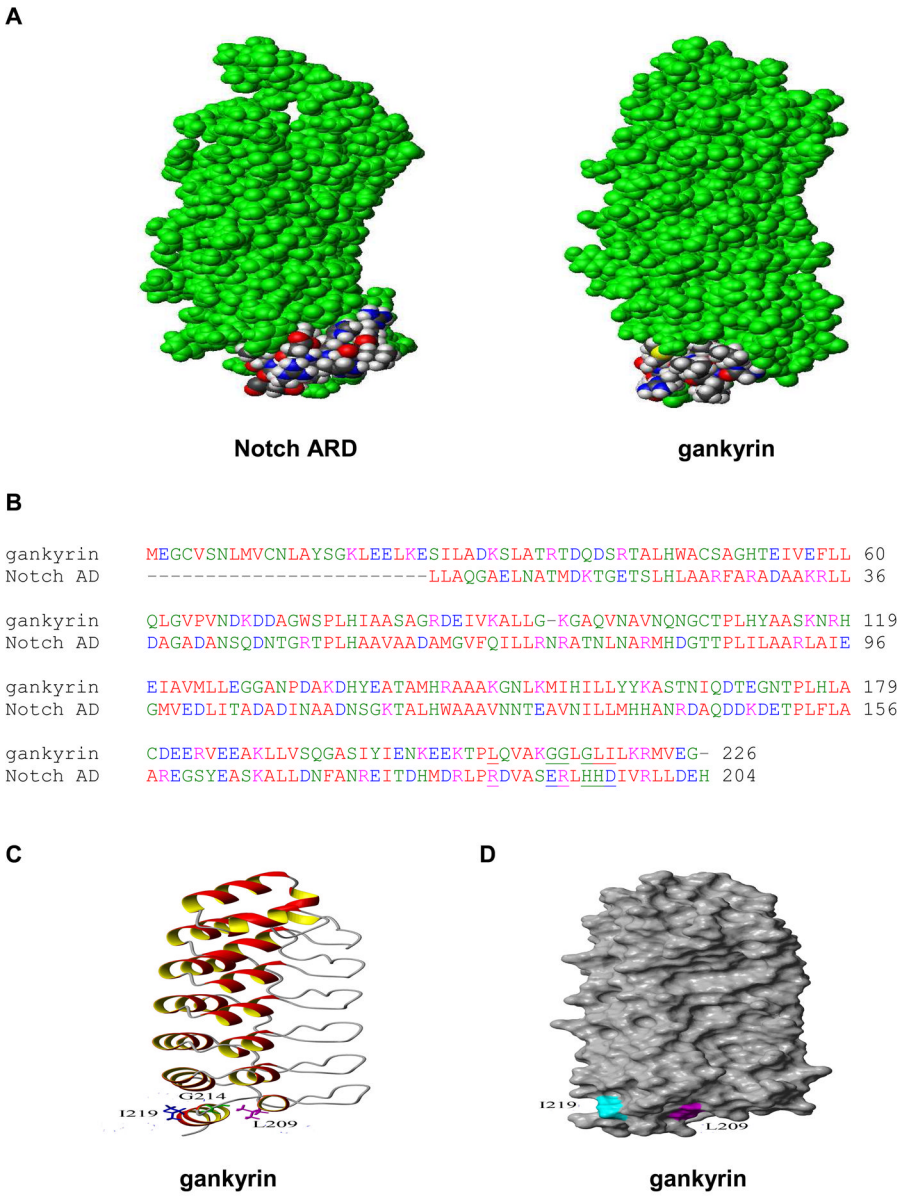

Figure 3. Homology and structure comparisons of human gankyrin and Notch ARD

A, Structural comparisons of human gankyrin (PDB ID: 1TR4) and Notch ARD (PDB ID: 1OT8). Charged residues located at the C-termini of gankyrin and Notch ARD were highlighted (28). **B,** Sequence homology analysis using ClustalW (www.expasy.com). Residues subjected to mutagenesis are underlined. **C,** Ribbon diagram of gankyrin showing residues L209 (magenta), G214 (green), and I219 (blue) in the C-terminal AR. It is noted that the side chain of L209 is located between the anti-parallel helices of the 7th AR and is engaged in helix-helix packing through interacting with the side chains of K220 and L221, In contrast, the side chain of L219 is largely solvent-exposed. **D,** Solvent accessible surface of gankyrin with L209 and I219 painted in magenta and cyan, respectively. The percentages of the solvent-accessible side chain surface are 32% and 55%, respectively, for L209 and I219. In **A, C,** and **D,** the N-termini are located at the top and the C-termini are at the bottom.

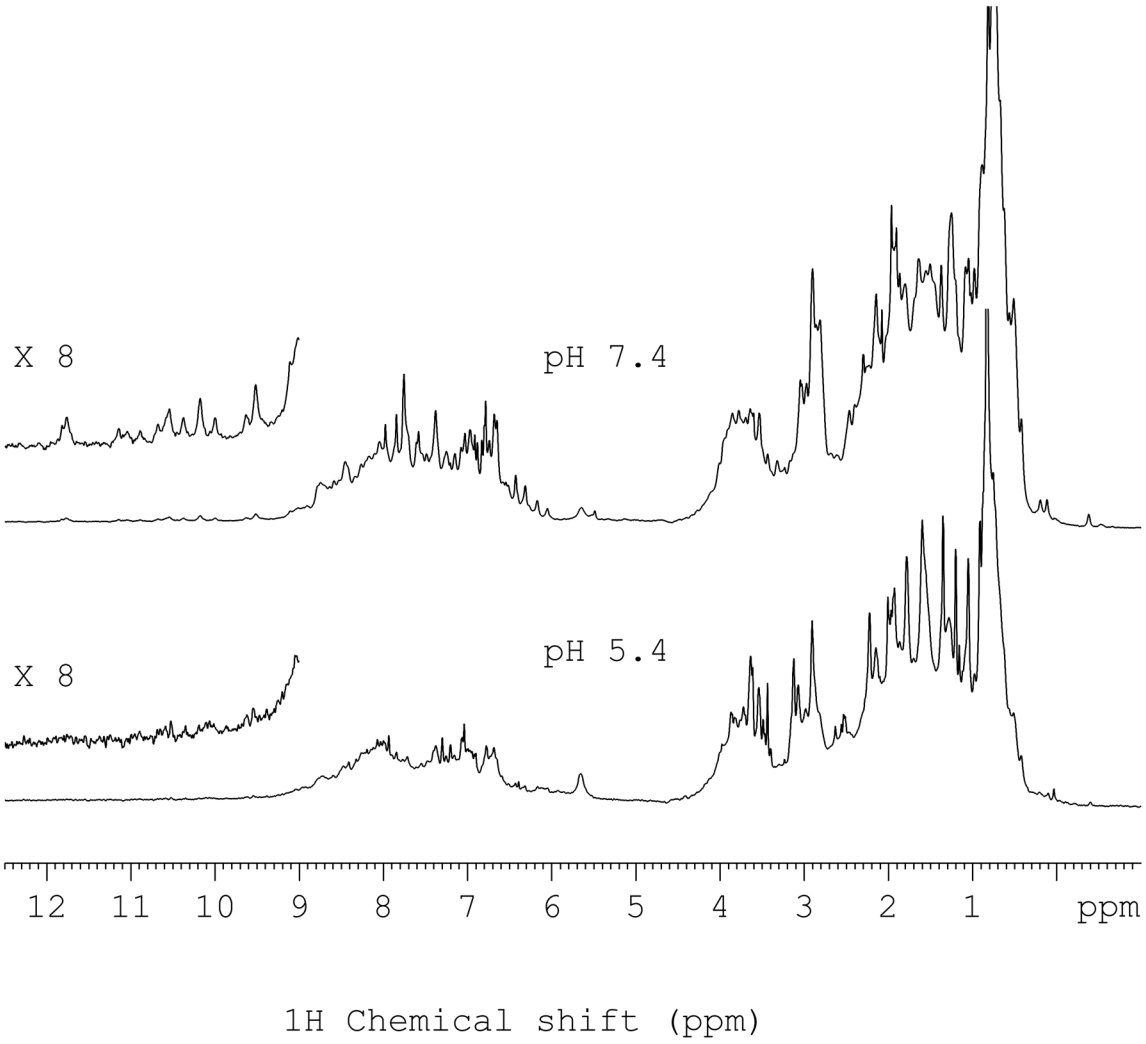

Figure 4. 1D ^{1}H NMR spectra on mutant Q210H at pH 5.4 and pH 7.4, respectively

The inserts are blow-up showing the downfield region that contains the signals of $H^{\varepsilon 2}$ from histidine residues in TPLH motifs.

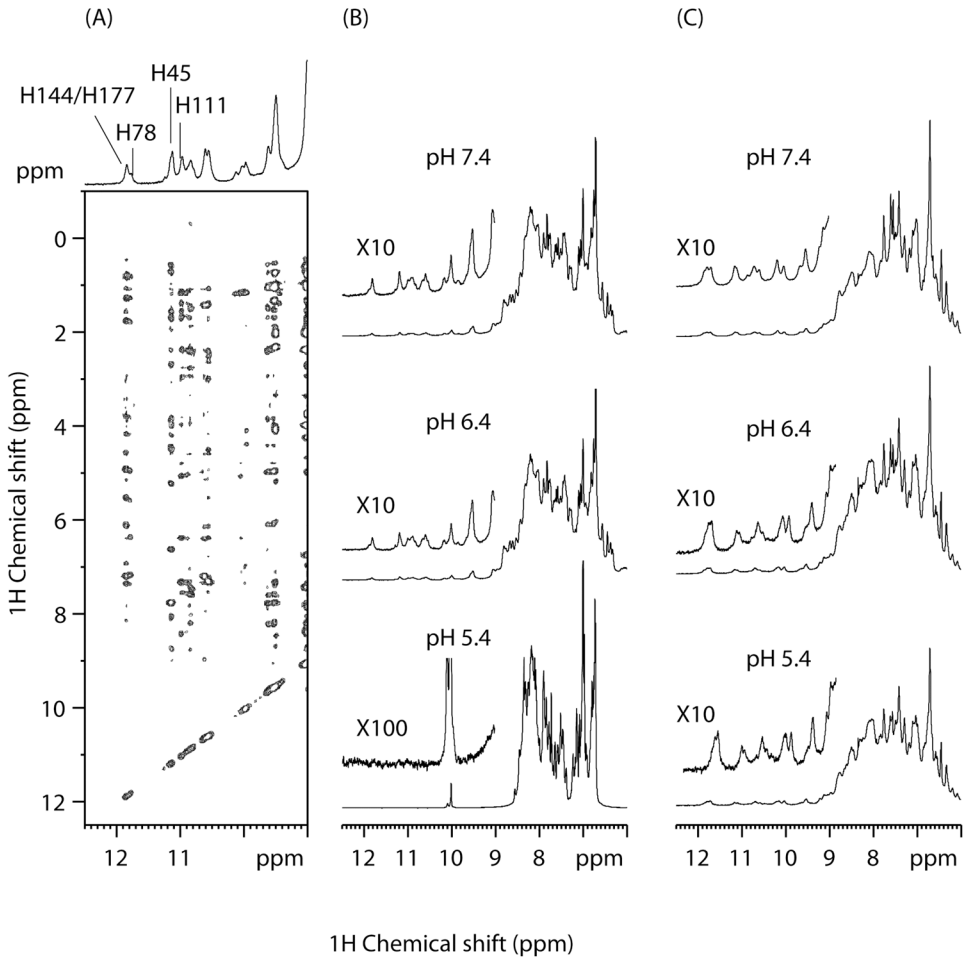

Figure 5. NMR studies showing that the removal of the C-terminal AR destabilized the tertiary structure of Gank$^{1-201}$ at acidic pH

A, Downfield region of the 2D NOESY recorded on Gank$^{1-201}$ at pH 7.4. The top projection shows the assignments of the histidine H$^{\varepsilon 2}$ protons in TPLH and its variant. **B,** 1D ^{1}H NMR of the amide region recorded on Gank$^{1-201}$ at pH 5.4, 6.4, and 7.4 after a week of incubation. **C,** 1D ^{1}H NMR of the amide region recorded on gankyrin WT at pH 5.4, 6.4, and 7.4 in the parallel experiments. In both **B** and **C,** the inserts are the blowup of the region between 9.00 and 12.50 ppm.

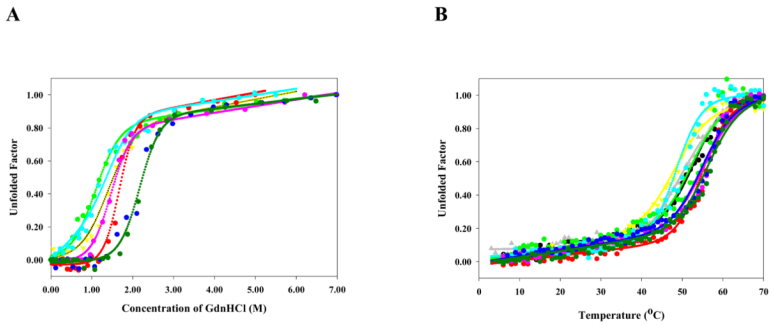

Figure 6. Evaluation of the conformational stabilities of gankyrin missense mutants

A, Chemical-induced unfolding. **B,** Heat-induced unfolding. The experiments were conducted as described in Figure 1 except that the experimental pH was 7.4 and the temperature range for heat-induced unfolding was 5–70 °C since some gankyrin mutants might have higher stabilities than gankyrin WT. In both **A** and **B,** solid circles represent experimental data and the dotted lines are fitting curves. Green, L209R; red, G214E; cyan, G215R; pink, G217H; yellow, L218H; blue, I219D; G215R/I219D, dark green.

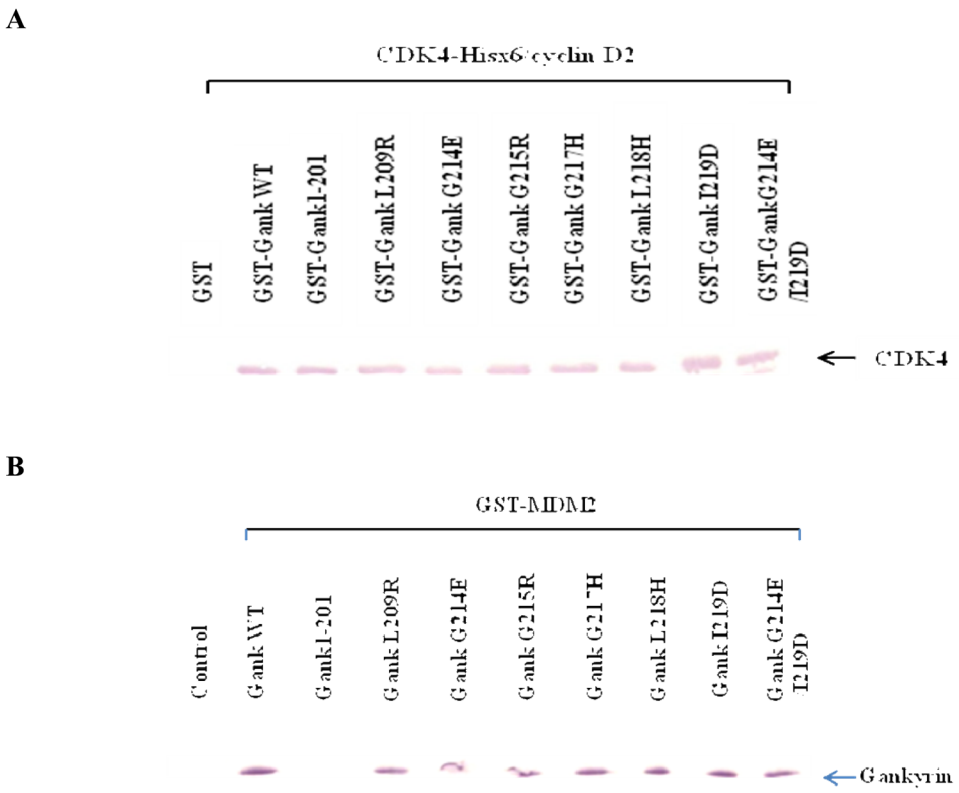

Figure 7. Pull-down assays to assess the mutagenic effect on gankyrin's function

A, Effect on the interaction between gankyrin and the CDK4-cyclin D2 complex (14). The reaction mixtures containing GST gankyrin proteins (~3.0 μM) and the $(His)_6$-tagged CDK4/cyclin D2 holoenzyme (~0.3 μM) were incubated with G beads. After washing with PBS, bound proteins were eluted out using reduced glutathione and blotted with anti- human CDK4 antibody. GST was used as a negative control. **B.** Effect on the interaction between gankyrin and MDM2. The experiments were performed as described in **A** except that the reaction mixtures containing free gankyrin proteins (~3.0 μM) and GST-MDM2 (~0.3 μM) and the pull-down products were blotted with a primary antibody again human gankyrin. The control reaction contained free gankyrin WT (~3.0 μM) and GST (~0.3 μM).

Table 1

The conformational stabilities of gankyrin proteins

	ΔG_d^{water} (kcal*mol^{-1})[a]	*m* (kcal*mol^{-1}*M^{-1})[a]	$D_{1/2}$ (M)[a]	Tm (°C)[a]
Wild type, pH 8.4	2.65	1.75	1.51	44.3
Wild type, pH 7.4	2.72	1.81	1.52	51.2
Wild type, PH 6.4	3.15	2.05	1.53	47.4
Wild type, pH 5.4	3.55	2.13	1.64	46.8
Gankyrin1-201, pH 8.4	1.95	1.75	1.12	44.0
Gankyrin1-201, pH 7.4	2.10	1.72	1.22	49.4
Gankyrin1-201, pH 6.4	2.45	1.70	1.44	50.9
Gankyrin1-201, pH 5.4	0.55	1.30	0.42	35.3
Q210H, pH 8.4	1.97	1.52	1.30	49.0
Q210H, pH 7.4	2.32	1.58	1.47	49.9
Q210H, pH 6.4	0.95	1.63	0.58	ND[c]
L209R, pH 7.4	2.10	1.95	1.08	49.5
G214E, pH 7.4	5.12	2.99	1.71	54.0
G215R, pH 7.4	2.75	1.86	1.49	47.8
G217H, pH 7.4	3.51	2.40	1.46	53.2
L218H, pH 7.4	2.43	1.75	1.39	50.5
I219D, pH 7.4	4.61	2.32	1.99	54.2
G214E/I219D, pH 7.4	5.25	2.35	2.23	55.1

[a] ΔG_d^{water}, $D_{1/2}$, and *m* values were calculated according to a two-state transition model (27), and the error in ΔG_d^{water} is estimated to be ± 0.2 kcal*mol^{-1}. Tm was defined as the temperature at the midpoint of transition, and the error is estimated to be ± 0.5 °C (12).

[c] ND, not determined. Tm of R210H at pH 6.4 was not determined due to the fact that after heat-induced unfolding, the refolding process was not recorded, i.e. the thermo-induced folding/unfolding of R210H at pH 6.4 was not reversible.